RESEARCH ARTICLE

Figures and figure supplements

Zika virus remodels and hijacks IGF2BP2 ribonucleoprotein complex to promote viral replication organelle biogenesis

Clément Mazeaud *et al*.

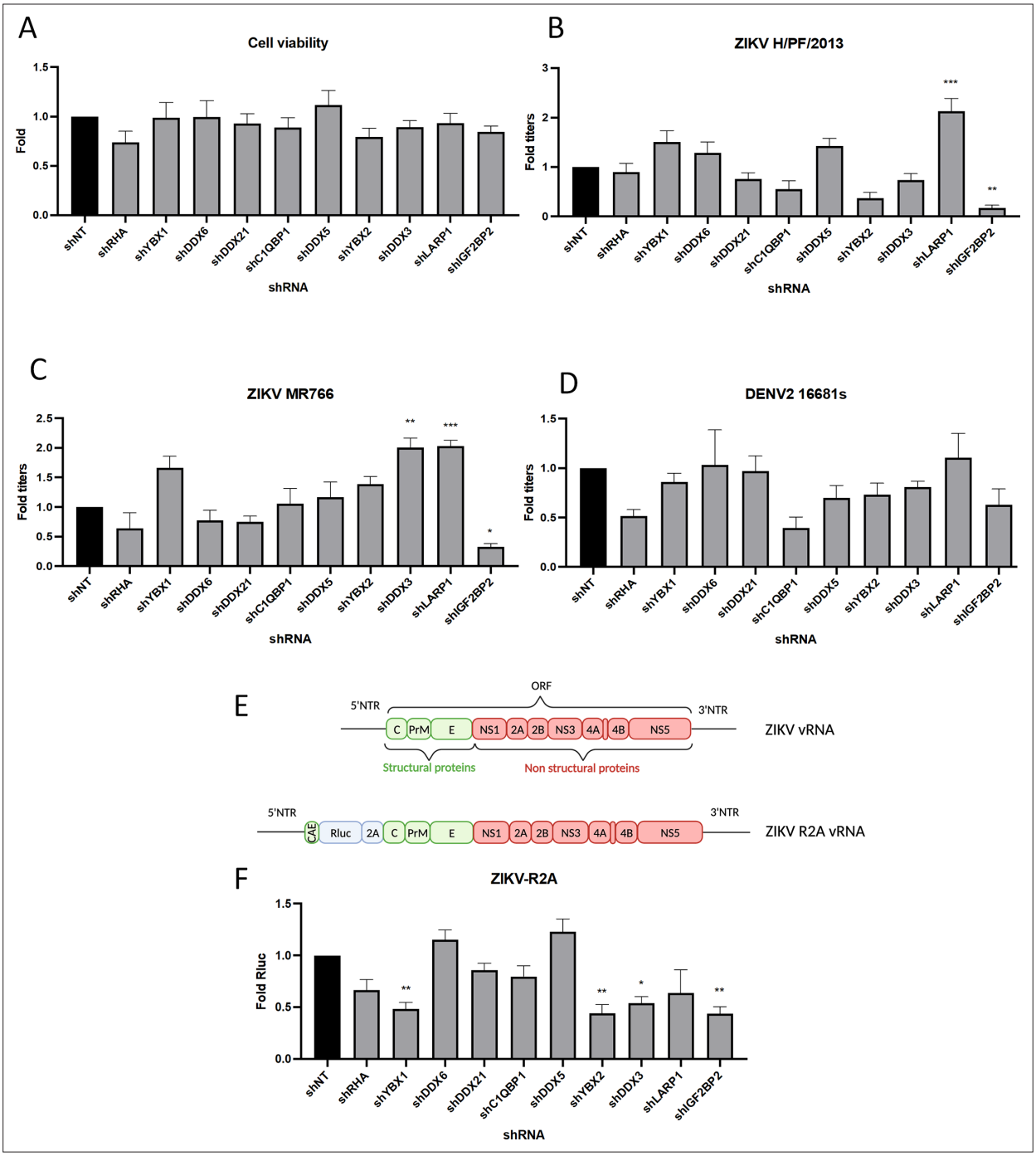

Figure 1. A RNA interference (RNAi) mini-screening of RNA-binding proteins to identify host factors involved in dengue virus (DENV) and Zika virus (ZIKV) replications. Huh7.5 were transduced with short-hairpin RNA (shRNA)-expressing lentiviruses at an MOI of 5–10. (**A**) Four days post-transduction, 3-(4,5-dimethylthiazol-2-yl)-2,5-diphenyltetrazolium bromide (MTT) assays were performed to evaluate cytotoxicity effect of the knockdown (KD). Two days post-transduction cells were infected with either (**B**) ZIKV H/PF/2013, (**C**) ZIKV MR766, or (**D**) DENV2 16681s at an MOI of 0.01. 48 hr post-infection, the production of infectious viral particles was evaluated by plaque assays. (**E**) Schematic of the Renilla luciferase (Rluc)-expressing ZIKV reporter virus (ZIKV-R2A) based on the FSS13025 isolate (Asian lineage). (**F**) Cells were prepared, exactly as in B–D but infected with ZIKV-R2A at an MOI of 0.001. 48 hr post-infection, cells were lysed and bioluminescence was measured and normalized to the control cells expressing a non-target shRNA (shNT). Means ± SEM are shown based on three to five independent experiments for each shRNA. p<0.0001; ***: p<0.001; **: p<0.01; *p<0.05 (one-way ANOVA test).

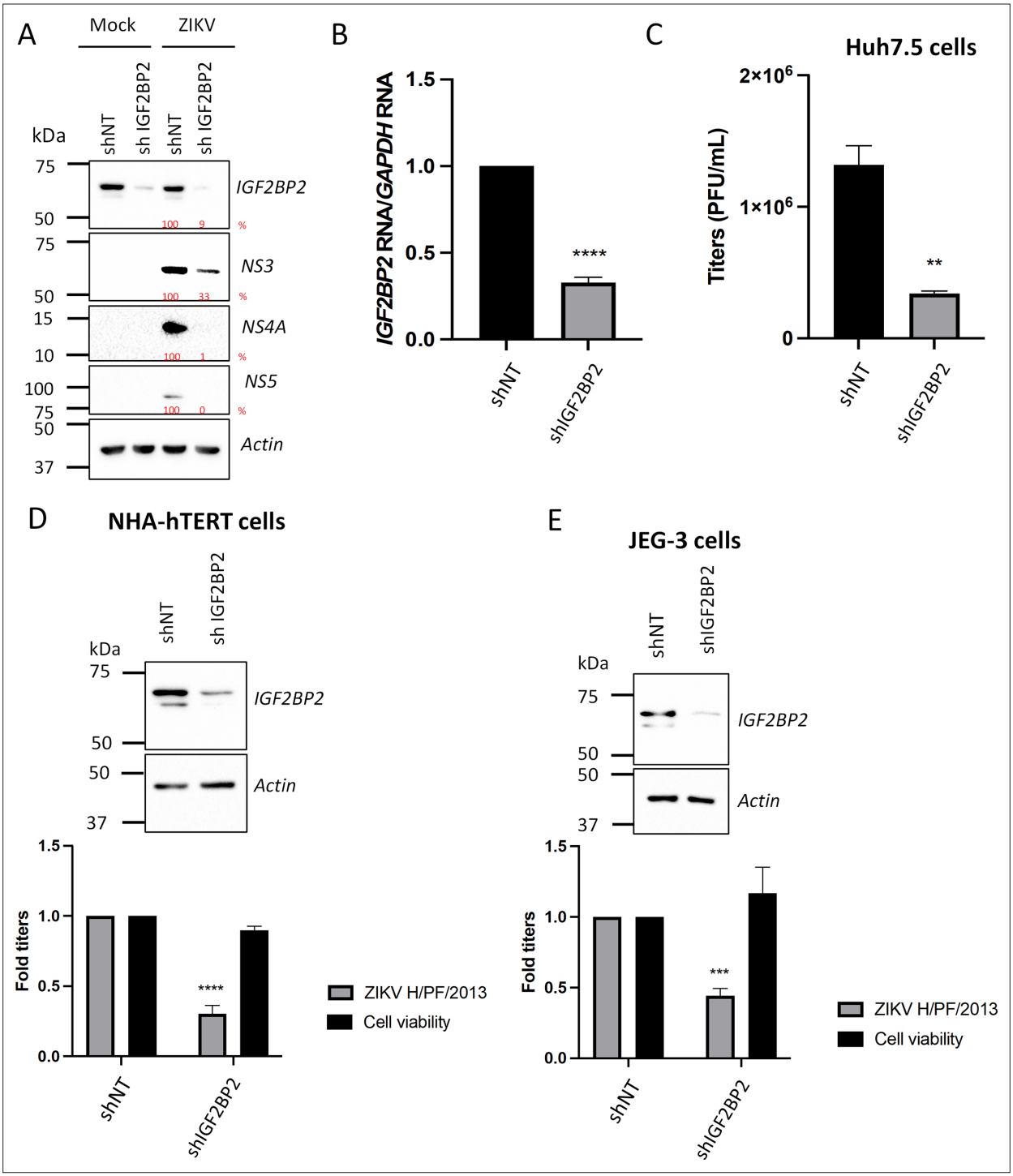

Figure 2. IGF2BP2 positively regulates Zika virus (ZIKV) replication in multiple cell lines. Liver Huh7.5 (**A–C**), astrocytic NHA-hTERT (**D**), and placental JEG-3 (**E**) cells were transduced with non-target shRNA (shNT) or shIGF2BP2 lentiviruses at an MOI of 10. Two days post-transduction, cells were infected with ZIKV H/PF/2013 at an MOI between 0.01 and 1 depending on the cell line. Two days post-infection, supernatant and cells were collected. IGF2BP2 expression at the protein level (A, D, E; all cell lines) and mRNA level (B; Huh7.5 cells) were evaluated by western blotting (WB) and RT-qPCR, respectively. Cell supernatants were used for plaque assays (**C–E**). For NHA-hTERT and JEG-3, the supernatant and cells are collected for titration and WB, respectively (**E–F**). 3-(4,5-Dimethylthiazol-2-yl)-2,5-diphenyltetrazolium bromide (MTT) assays were performed to assess the cell viability in transduced NHA-hTERT and JEG-3 cells (**D–E**). Means ± SEM are shown based on five (**D**), three (**C**), and four (**D–E**) independent experiments. ****: p<0.0001; ***: p<0.001; **: p<0.01 (unpaired t-test).

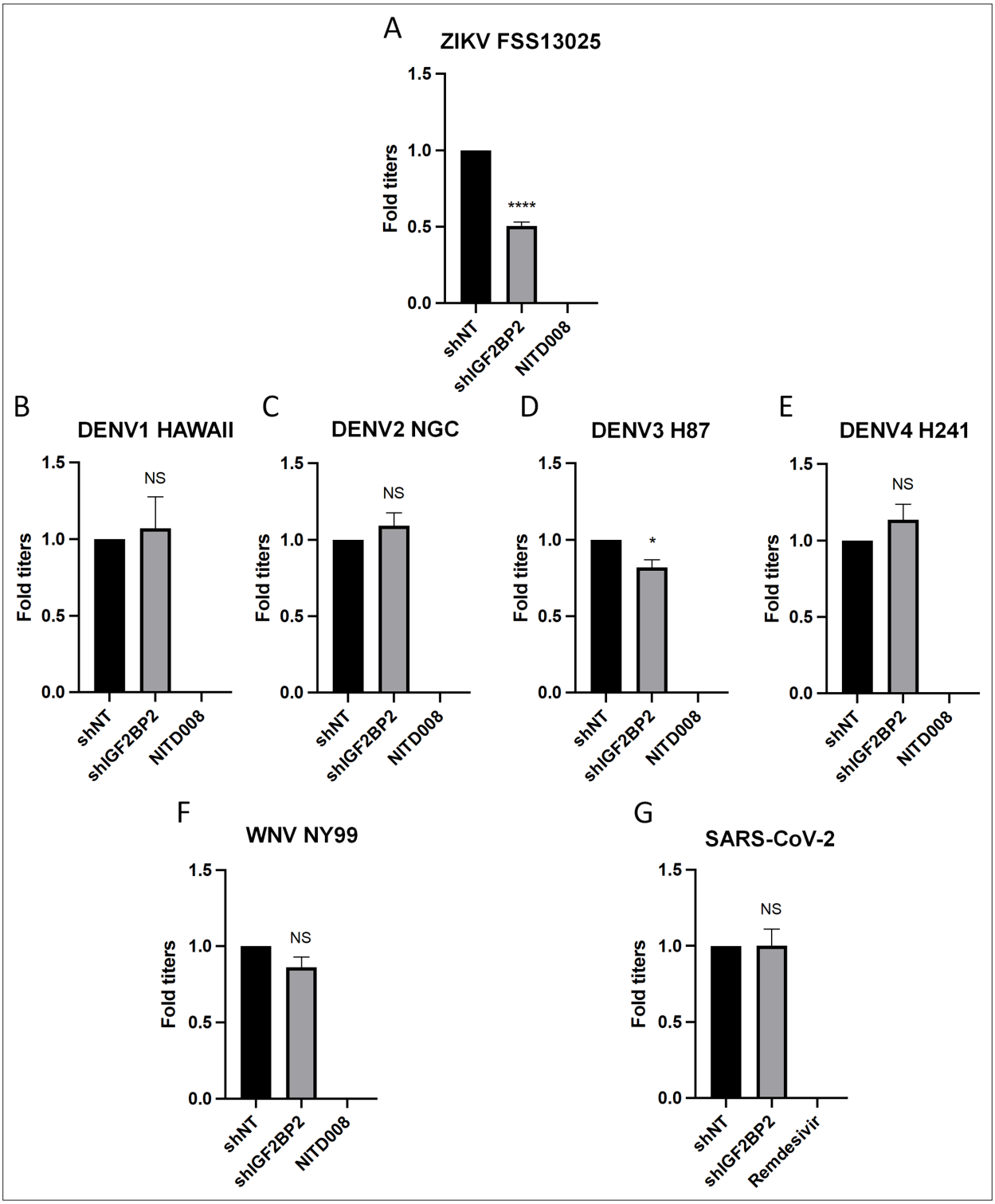

Figure 3. IGF2BP2 dependency is Zika virus (ZIKV)-specific. Huh7.5 cells were transduced with non-target shRNA (shNT) or shIGF2BP2 lentiviruses at an MOI of 10. Two days post-transduction cells were infected with (**A**) ZIKV FSS13025, (**B**) dengue virus (DENV)1 HAWAII, (**C**) DENV2 NGC, (**D**) DENV3 H87, (**E**) DENV4 H241, (**F**) West Nile virus (WNV) NY99, (**G**) SARS-CoV-2 at an MOI of 0.1. Virus-containing cell supernatants were collected and titrated 2 days post-infection by plaque assays. Treatment with RNA-dependent RNA polymerase (RdRp) inhibitors NITD008 and Remdesivir were used as positive controls of replication inhibition of orthoflaviviruses and SARS-CoV-2, respectively. Means ± SEM are shown based on three independent experiments. ****: $p<0.0001$; *: $p<0.05$; NS: not significant (unpaired t-test).

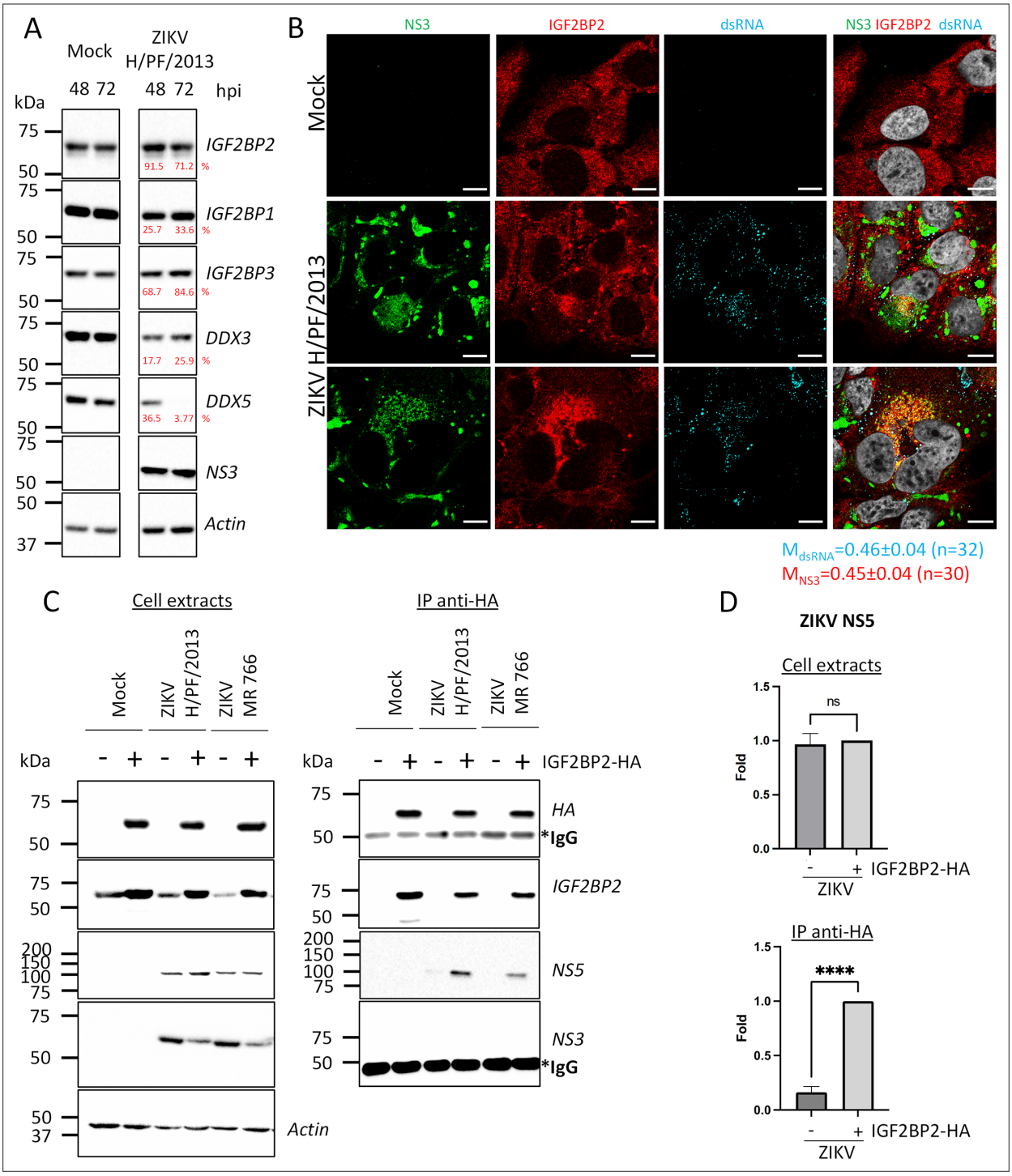

Figure 4. IGF2BP2 associates with NS5 and accumulates into Zika virus (ZIKV) replication compartment. (**A**) Huh 7.5 cells were infected with ZIKV H/PF/2013 at an MOI of 5. Cells were collected at 48 and 72 hr post-infection (hpi). Cell extracts were prepared and analyzed by western blotting using the indicated antibodies. Actin-normalized protein signals are shown. (**B**) Huh7.5 cells were infected with ZIKV H/PF/2013 with an MOI of 10 or left uninfected. Two days post-infection, cells were fixed, immunolabeled for the indicated factors, and imaged by confocal microscopy. Scale bar = 10 µm. The Manders' coefficient (mean ± SEM) representing the fraction of dsRNA (cyan) and NS3 (red) signals overlapping with IGF2BP2 signal is shown (n=number of cells). (**C**) Co-immunoprecipitation assays using HA antibodies were performed with extracts from Huh7.5 cells stably expressing IGF2BP2-HA (+) or control-transduced cells (-) which were infected with ZIKV at an MOI of 10 for 2 days. Purified complexes were analyzed for their protein content by western blotting. (**D**) Means of quantified NS5 signals from (C) (normalized to actin [extracts] or IGF2BP2 [IP]) ± SEM are shown based on nine independent experiments. ****: p<0.0001; ns: not significant (unpaired t-test).

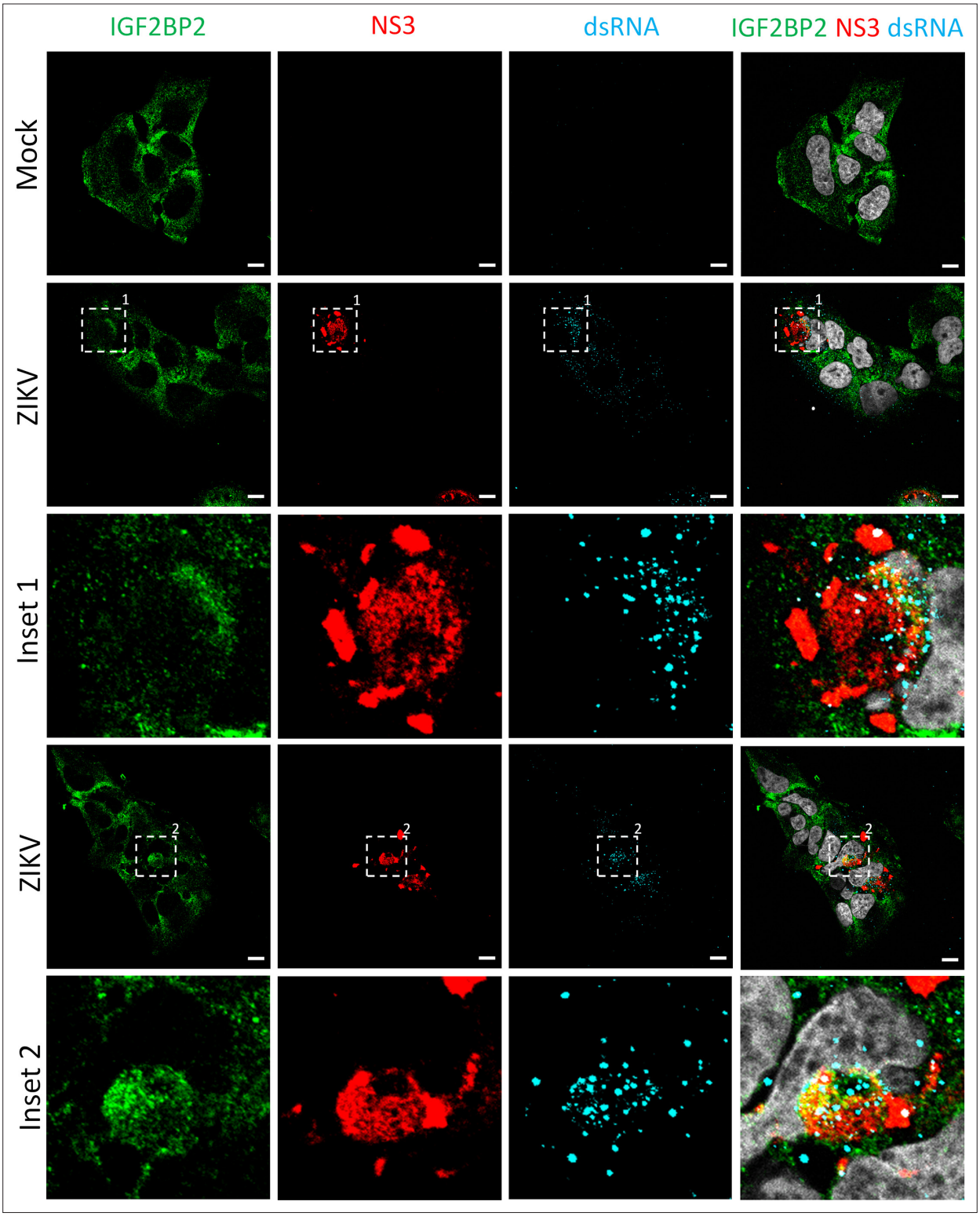

Figure 4—figure supplement 1. IGF2BP2 relocalizes to the viral replication compartment in Zika virus (ZIKV)-infected cells at 1 day post-infection. Huh7.5 cells were infected with ZIKV H/PF/2013 with an MOI of 10 or left uninfected. At 1 day post-infection, cells were fixed, immunolabeled for the indicated factors, and imaged by confocal microscopy. Scale bar = 10 μm. The white squares indicate the magnified areas in the insets.

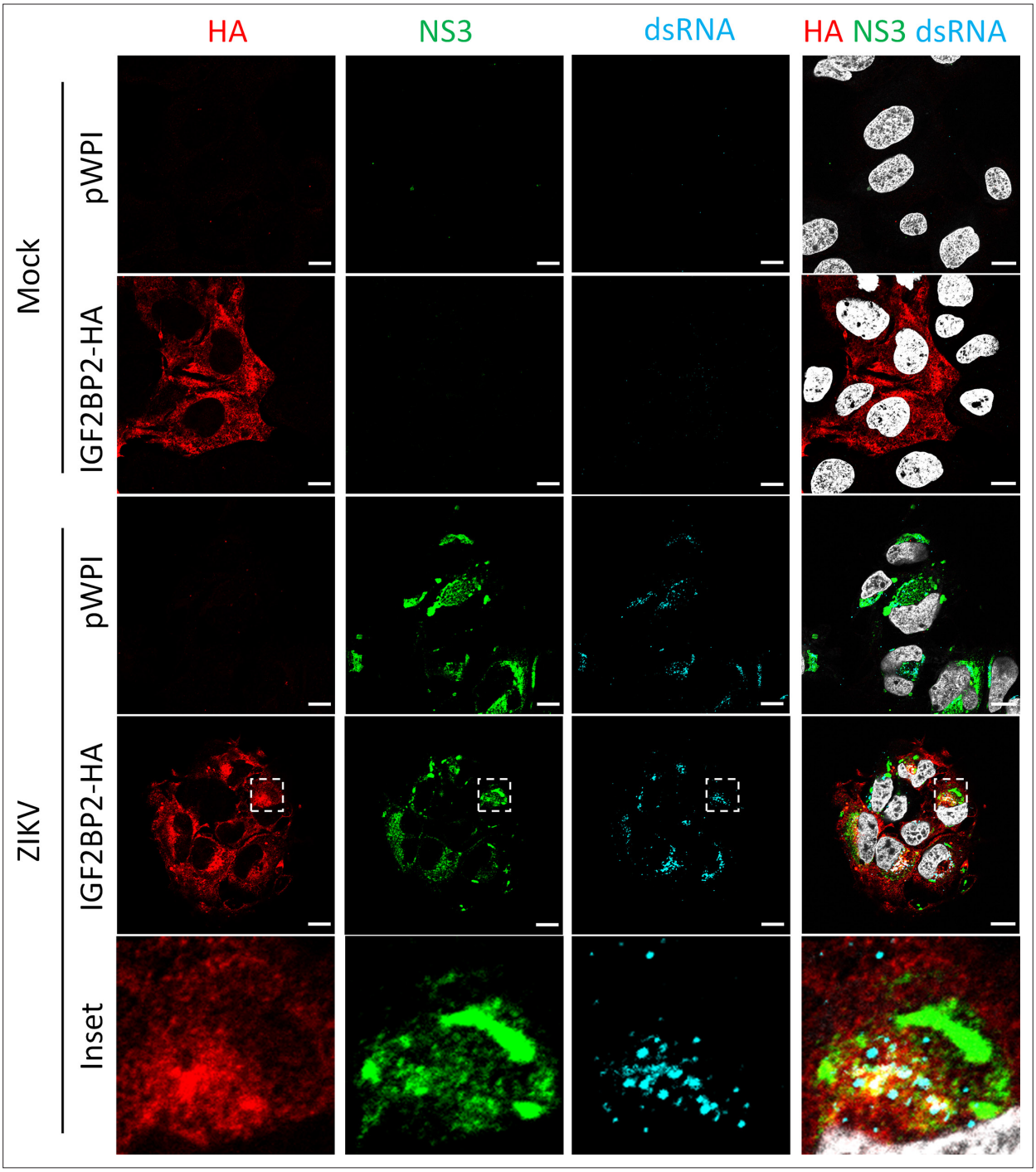

Figure 4—figure supplement 2. HA-tagged IGF2BP2 relocalizes to the viral replication compartment in Zika virus (ZIKV)-infected cells, as endogenous IGF2BP2. Huh7.5 cells stably overexpressing IGF2BP2-HA or control-transduced cells (pWPI) were infected with ZIKV H/PF/2013 with an MOI of 10 or left uninfected. Two days post-infection, cells were fixed, immunolabeled for the indicated factors, and imaged by confocal microscopy. Scale bar = 10 µm. The white squares indicate the magnified areas in the insets.

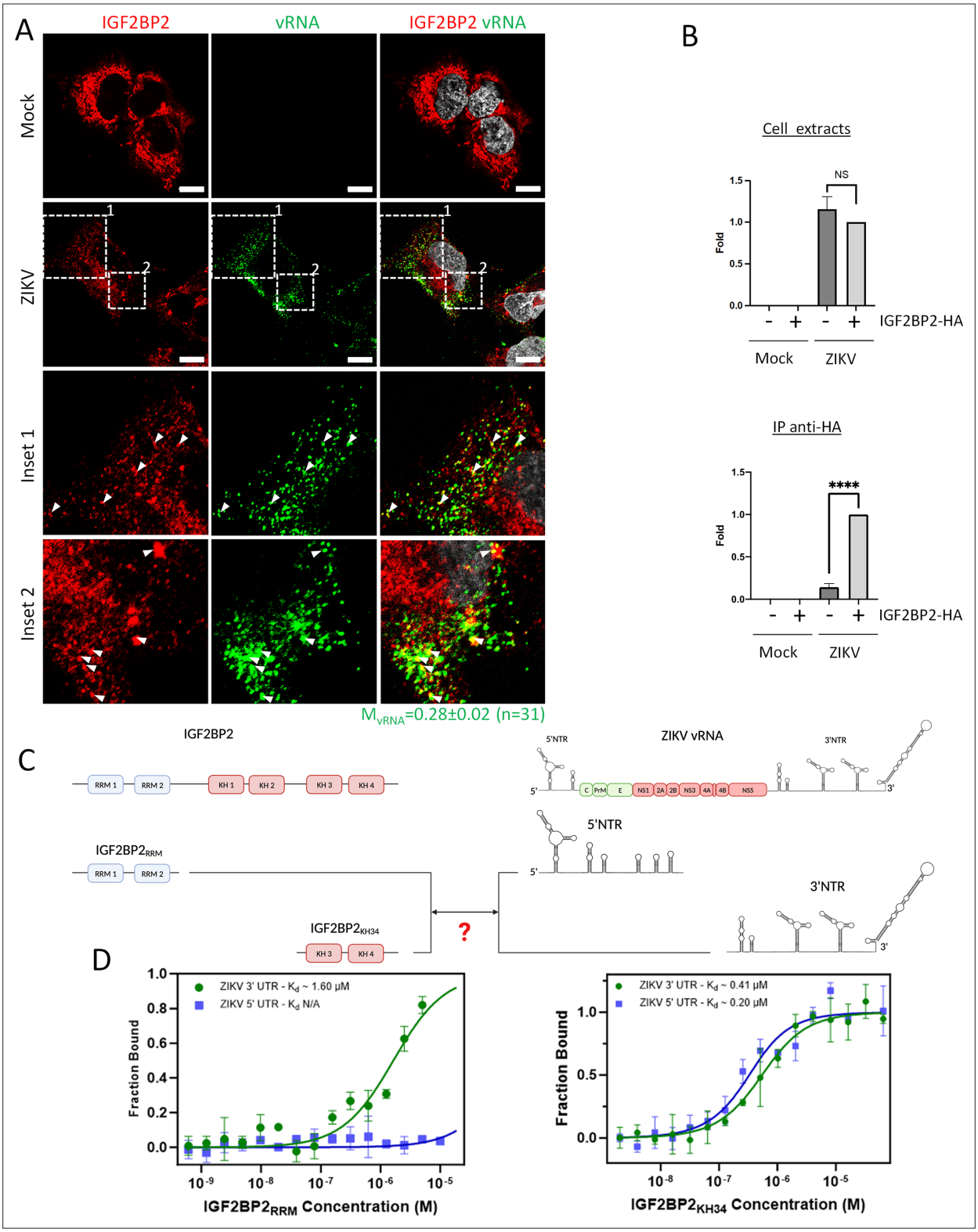

Figure 5. IGF2BP2 interacts with Zika virus (ZIKV) viral RNA (vRNA). (**A**) Fluorescence *in situ* hybridization (FISH) and IGF2BP2 immunostaining were performed using Huh 7.5 cells which were infected for 2 days with ZIKV (MOI = 10) or left uninfected. The Manders' coefficient (mean ± SEM) representing the fraction of vRNA signal overlapping with IGF2BP2 signal is shown (n=number of cells). Scale bar = 10 µm. (**B**) Huh7.5 cells expressing IGF2BP2-HA and control cells were infected with ZIKV H/PF/2013 at an MOI of 10, or left uninfected. Two days later, cell extracts were prepared and subjected to anti-HA immunoprecipitations. Extracted vRNA levels were measured by RT-qPCR. Means ± SEM are shown based on three independent

Figure 5 continued on next page

Figure 5 continued

experiments. ****: p<0.0001; NS: not significant (unpaired t-test). (**C**) IGF2BP2 recombinant proteins containing either the two RNA recognition motifs (RRM) or KH3 and KH4 domains were produced in bacteria and purified. In parallel ZIKV 5′ nontranslated region (NTR) and 3′ NTR were synthesized by *in vitro* transcription. (**D**) Combination of truncated IGF2BP2 proteins and either ZIKV 5′ NTR (blue squares) or ZIKV 3′ NTR (green circles) were used for *in vitro* binding assays using microscale thermophoresis.

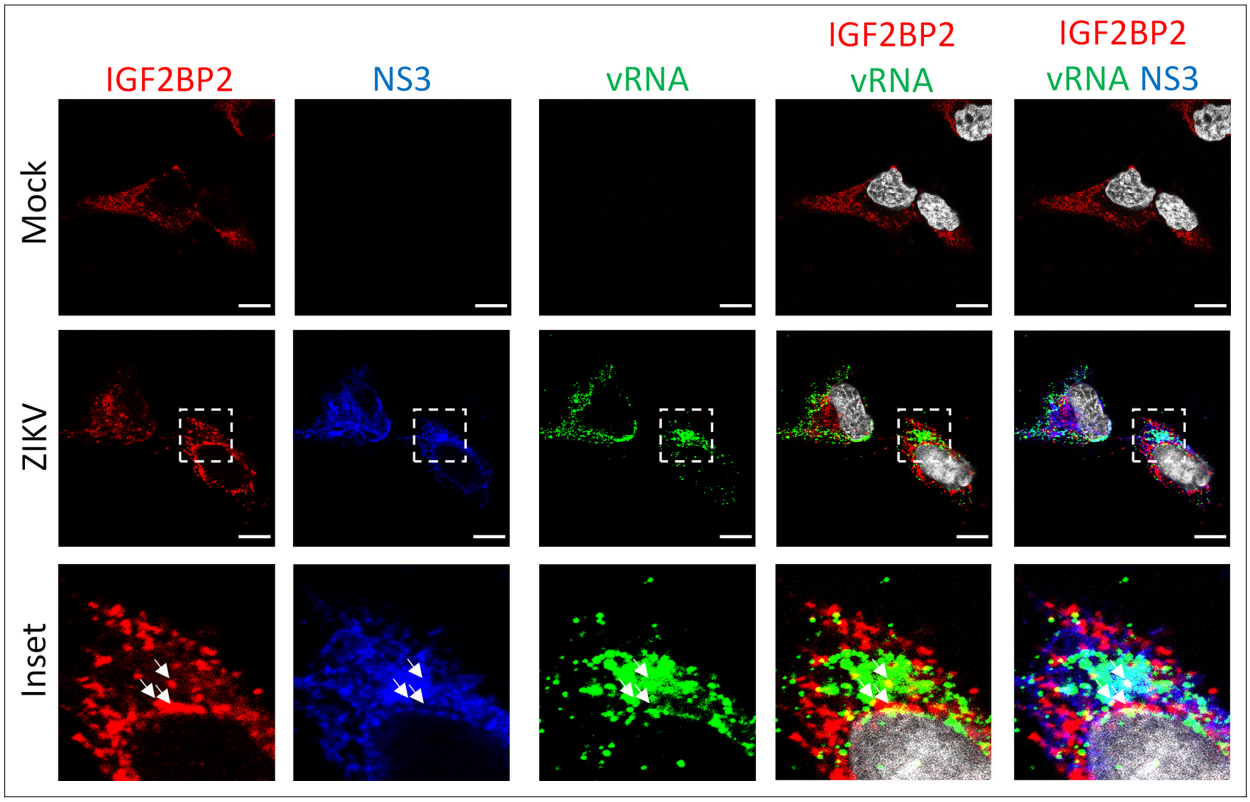

Figure 5—figure supplement 1. IGF2BP2 partially colocalizes with NS3 and viral RNA (vRNA) in Zika virus (ZIKV)-infected cells. Fluorescence *in situ* hybridization (FISH) with IGF2BP2 and NS3 co-immunostaining was performed in Huh7.5 cells after 2 days post-infection with ZIKV at an MOI of 10. White arrows show the triple colocalization. Scale bar = 10 µm. The white squares indicate the magnified areas in the insets.

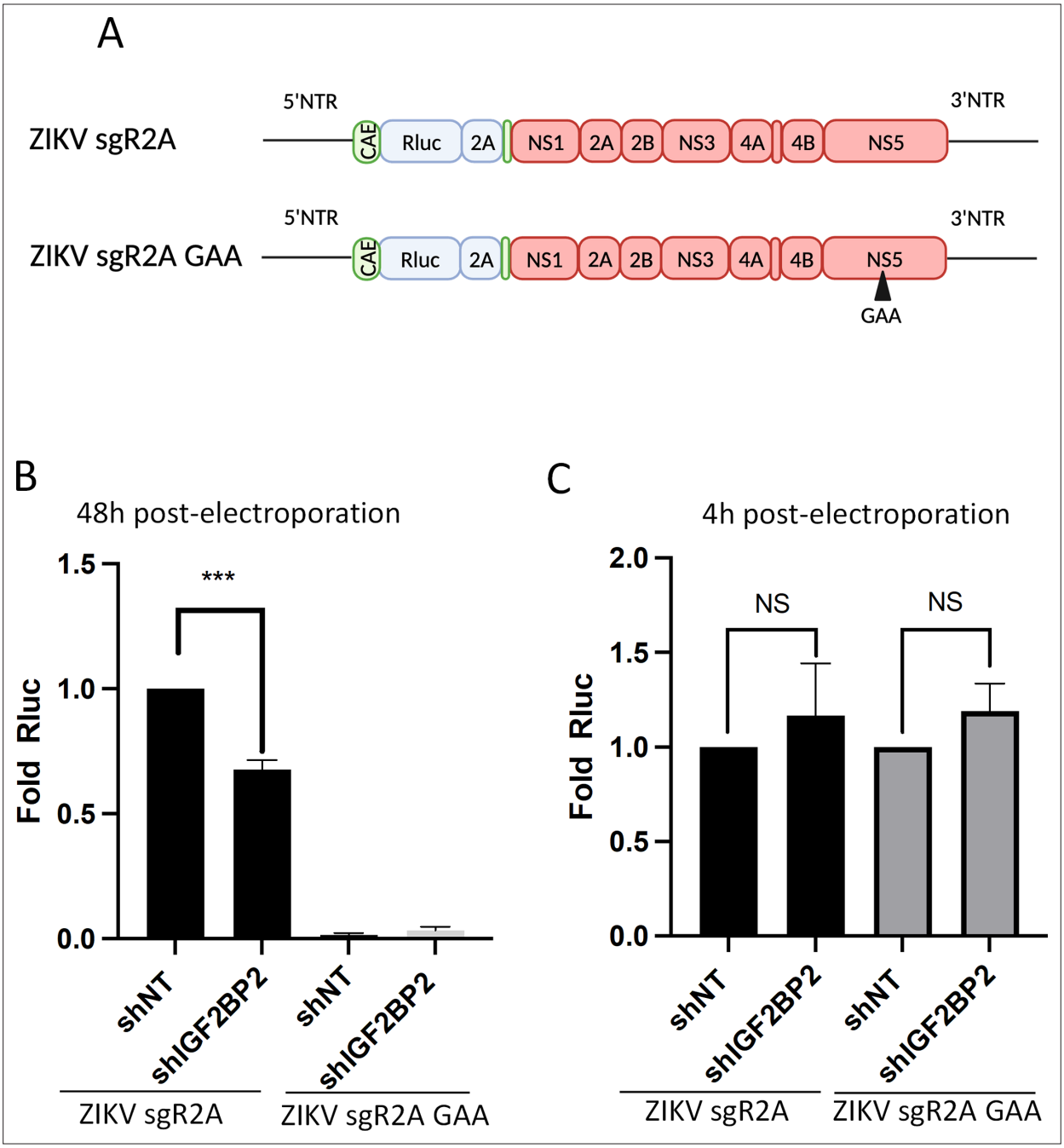

Figure 6. IGF2BP2 regulates the replication of Zika virus (ZIKV) viral RNA (vRNA). (**A**) Schematic representation of reporter ZIKV H/PF/2013 sub-genomic replicons (sgR2A) and replication-deficient genomes because of mutations in NS5 RNA-dependent RNA polymerase (RdRp) sequence (sgR2A GAA). (**B–C**) Huh7.5 were transduced with short-hairpin RNA (shRNA)-expressing lentiviruses and subjected to electroporation with *in vitro*-transcribed sgR2A or sgR2A GAA RNAs 2 days later. In-cell bioluminescence was measured (**B**) 48 or (**C**) 4 hr post-electroporation and normalized to the non-target shRNA (shNT) control condition. In (C), the luciferase activity was normalized to the transfection efficiency, i.e., the Renilla luciferase (Rluc) activity at 4 hr post-electroporation. Means ± SEM are shown based on four independent experiments. ***: p<0.001; NS: not significant (unpaired t-test).

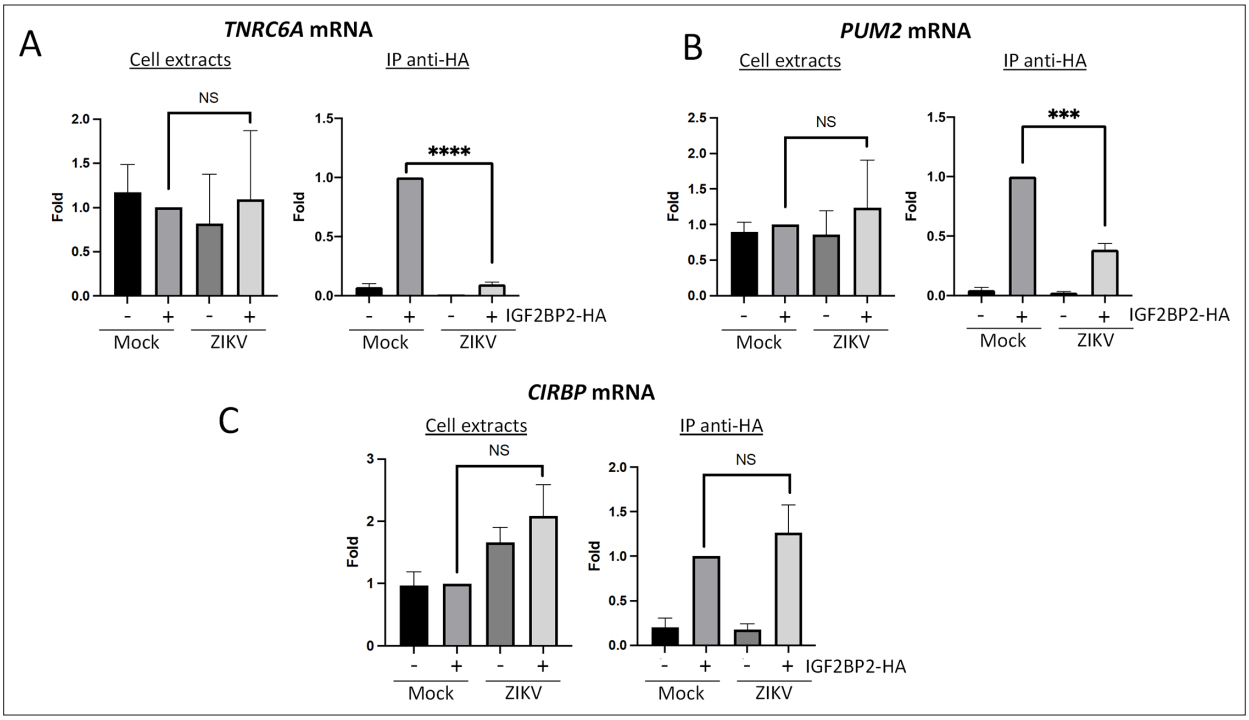

Figure 7. Zika virus (ZIKV) infection decreases the interaction between IGF2BP2 and several of its mRNA endogenous ligands. Huh7.5 cells stably expressing IGF2BP2-HA (+) and control cells (-) were infected with ZIKV H/PF/2013 at an MOI of 10, or left uninfected. Two days later, cell extracts were prepared and subjected to anti-HA immunoprecipitations. Extracted (**A**) *TNRC6A*, (**B**) *PUM2*, and (**C**) *CIRBP* mRNA levels were measured by RT-qPCR. Means ± SEM are shown based on three independent experiments. ****: p<0.0001; ***: p<0.001; NS: not significant (unpaired t-test).

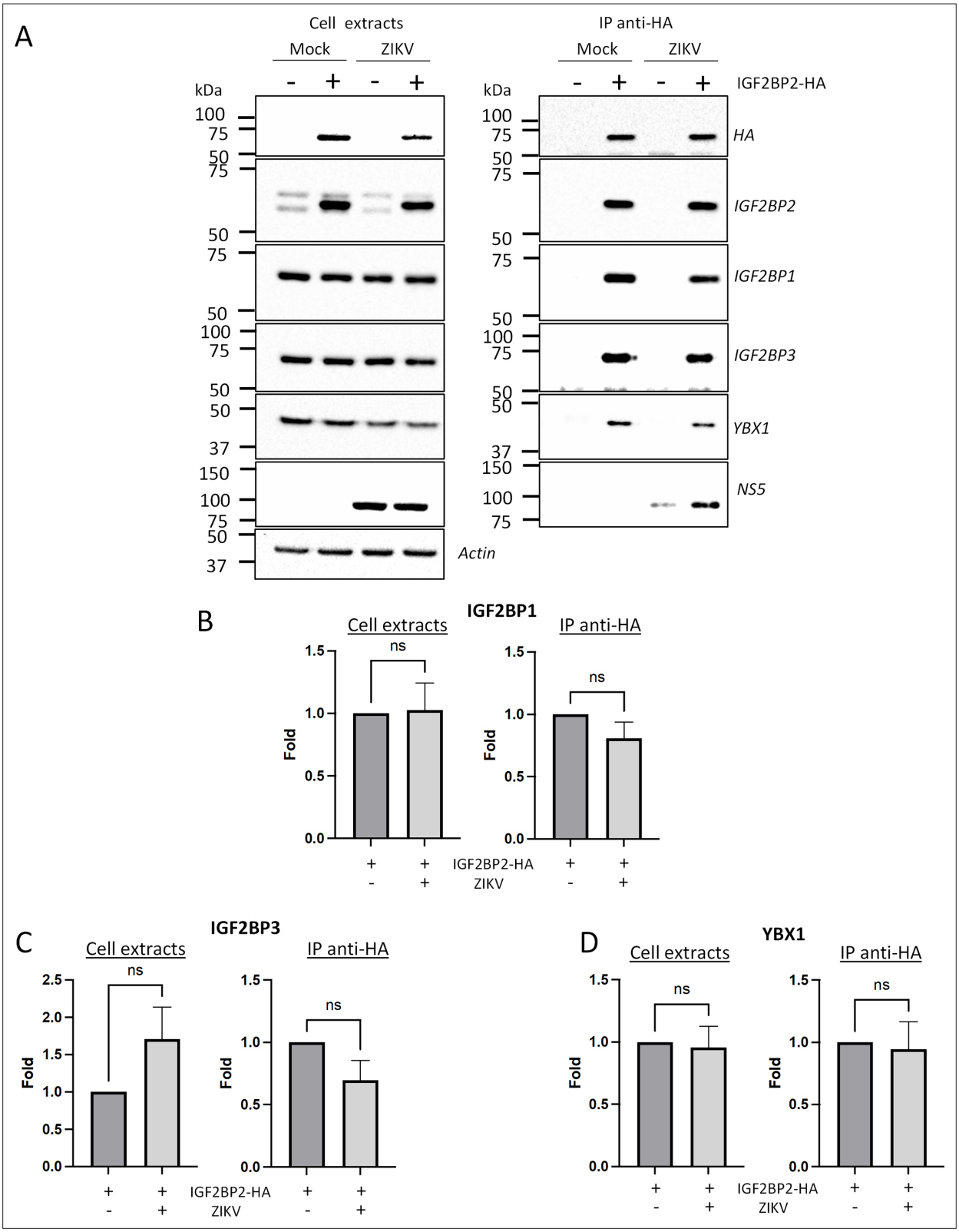

Figure 8. Zika virus (ZIKV) infection does not significantly impact the association of IGF2BP2 with IGF2BP1, IGF2BP3, and YBX1. Huh7.5 cells stably expressing IGF2BP2-HA (+) and control cells (-) were infected with ZIKV H/PF/2013 at an MOI of 10, or left uninfected. Two days later, cell extracts were prepared and subjected to anti-HA immunoprecipitations. (**A**) Purified complexes were analyzed by western blotting for their content in the indicated proteins. IGF2BP1 (**B**), IGF2BP3 (**C**), and YBX1 (**D**) levels were quantified and means of protein signals (normalized to actin [extracts] and IGF2BP2 [IP]) ± SEM are shown based on six to eight independent experiments. ns: not significant (unpaired t-test).

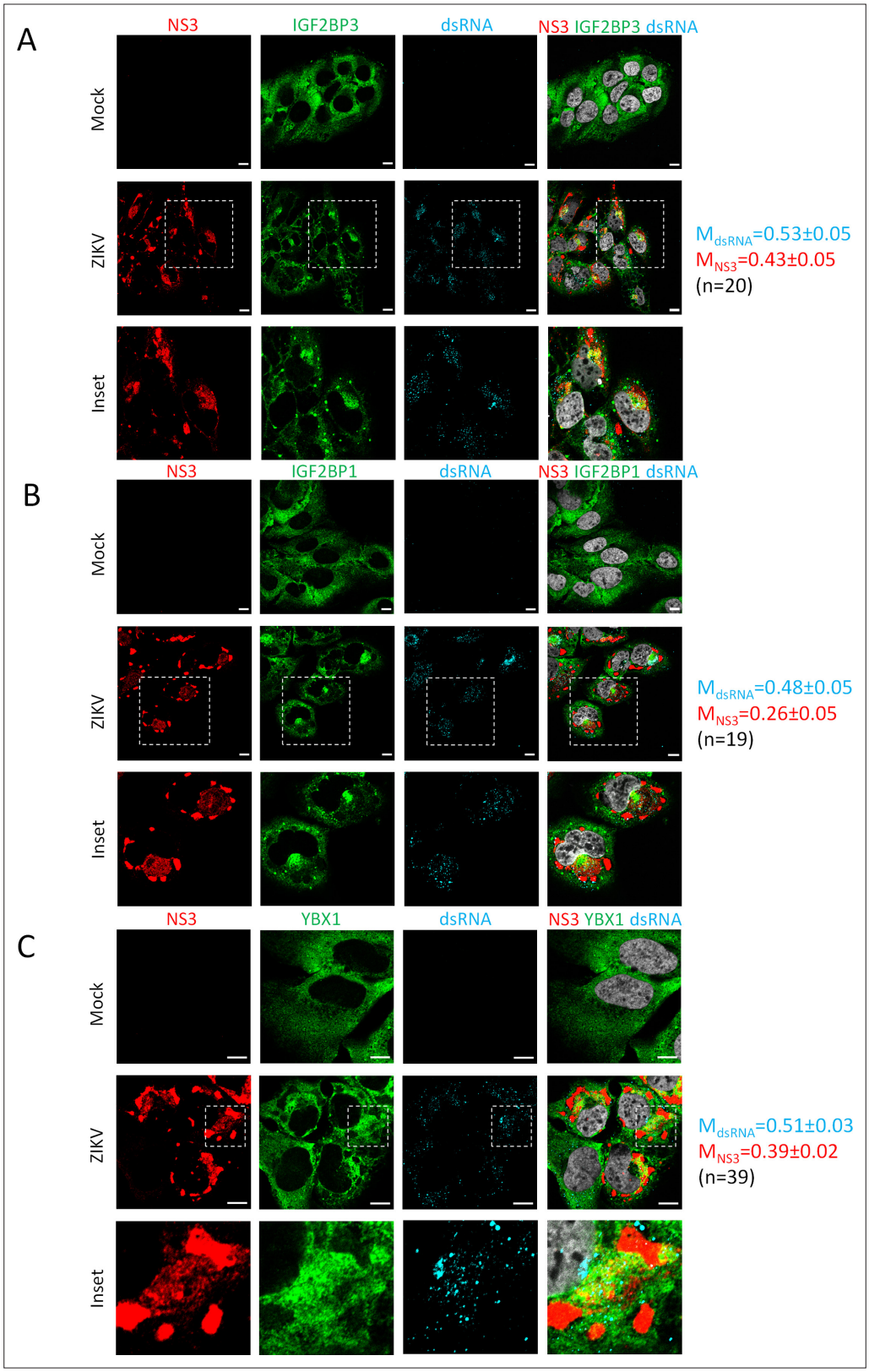

Figure 8—figure supplement 1. IGF2BP1, IGF2BP3, and YBX1 relocalize to the viral replication compartment in Zika virus (ZIKV)-infected cells. Huh7.5 cells were infected with ZIKV H/PF/2013 with an MOI of 10 or left uninfected. Two days post-infection, cells were fixed, immunolabeled for the indicated factors, and imaged by confocal microscopy. Scale bar = 10 µm. The Manders' coefficients (mean ± SEM) representing the fraction of dsRNA (cyan)

Figure 8—figure supplement 1 continued on next page

Figure 8—figure supplement 1 continued

and NS3 (red) signals overlapping with IGF2BP3 (**A**), IGF2BP1 (**B**), or YBX1 (**C**) signals are shown (n=number of cells). The white squares indicate the magnified areas in the insets.

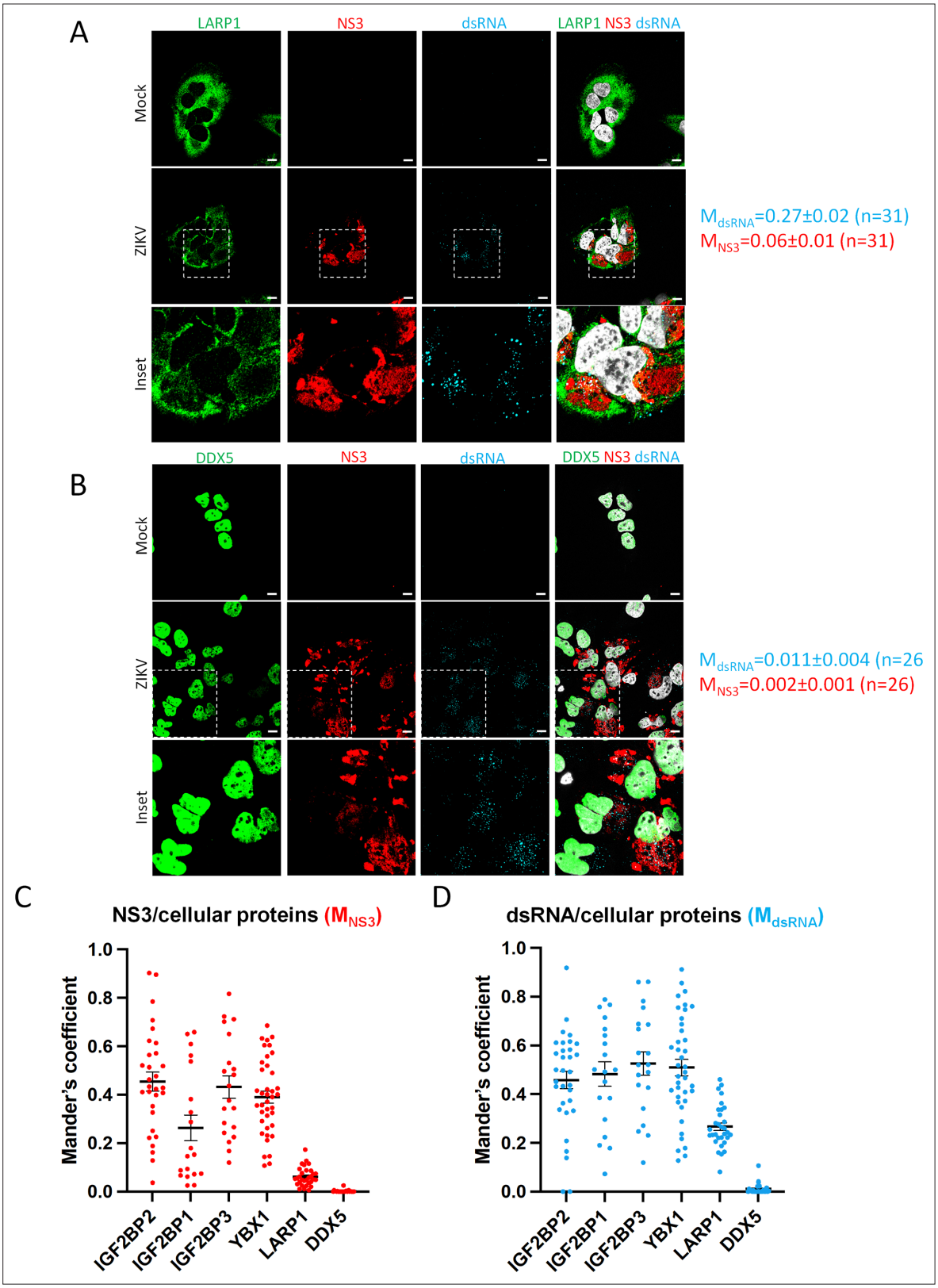

Figure 8—figure supplement 2. LARP1 and DDX5 do not relocalize to the viral replication compartment in Zika virus (ZIKV)-infected cells. (**A–B**) Huh7.5 cells were infected with ZIKV H/PF/2013 with an MOI of 10 or left uninfected. Two days post-infection, cells were fixed, immunolabeled for the indicated factors, and imaged by confocal microscopy. Scale bar = 10 µm. The Manders' coefficients (mean ± SEM) representing the fraction of double-stranded RNA (dsRNA) (cyan) and NS3 (red) signals overlapping with LARP1 (**A**) or DDX5 (**B**) signals are shown (n=number of cells). The white squares indicate the

Figure 8—figure supplement 2 continued on next page

Figure 8—figure supplement 2 continued

magnified areas in the insets. (**C–D**) The Manders' coefficients per cell determined from ***Figure 4B***, ***Figure 8—figure supplements 1A–C and 2A, B*** are plotted. Means ± SEM are shown in black.

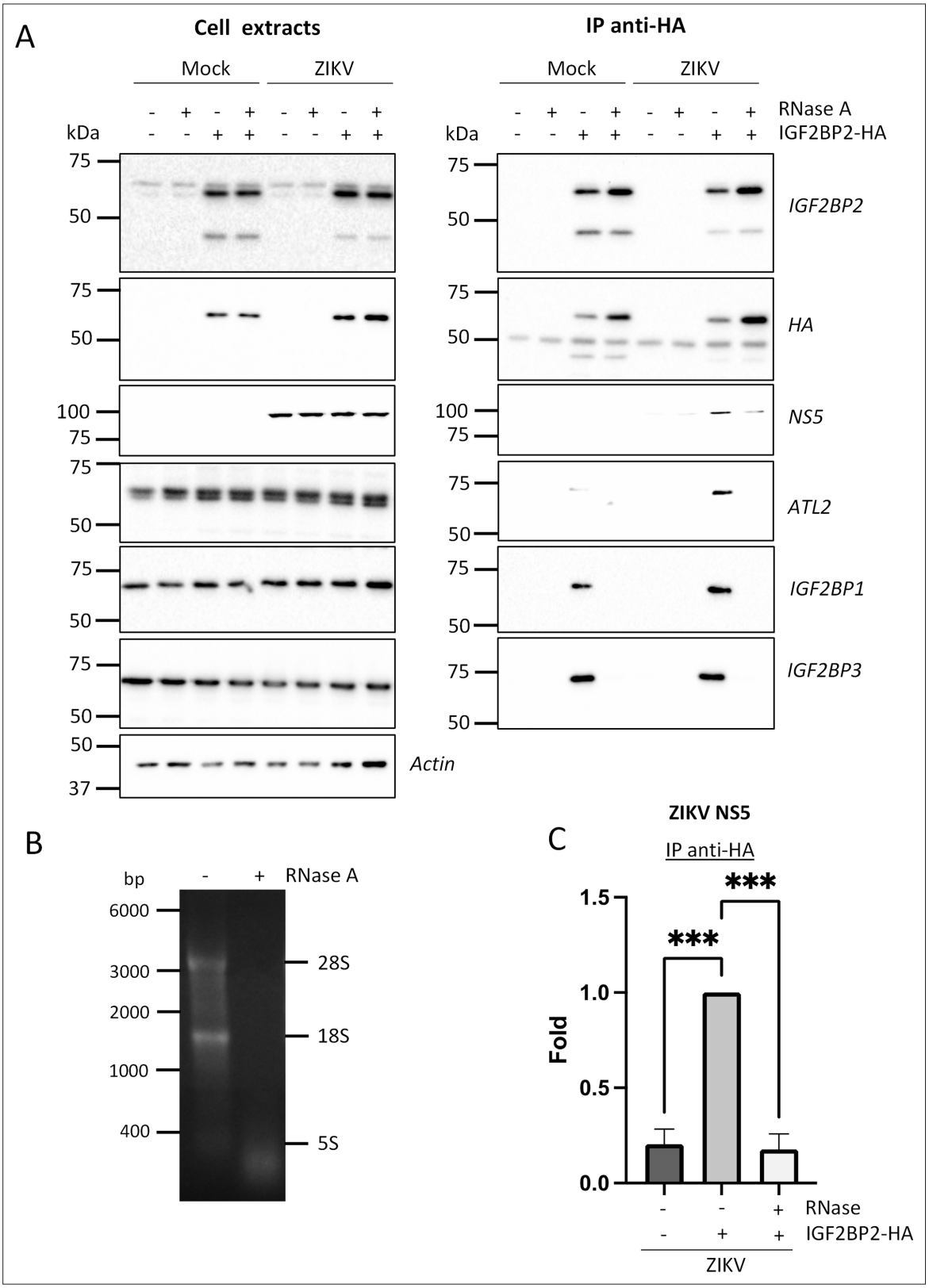

Figure 8—figure supplement 3. The association between IGF2BP2 and Zika virus (ZIKV) NS5 is RNA-dependent in infected cells. (**A**) Huh7.5 cells stably expressing IGF2BP2-HA (+) and control cells (-) were infected with ZIKV H/PF/2013 at an MOI of 10 or left uninfected. Two days later, cell extracts were prepared and subjected to RNase A treatment (+) or not (-) before anti-HA immunoprecipitations. The resulting complexes were analyzed by western blotting for their abundance in the indicated proteins. (**B**) The RNA content in cell extracts was analyzed on an agarose gel for controlling the efficiency

Figure 8—figure supplement 3 continued on next page

Figure 8—figure supplement 3 continued

of the RNase A treatment. (**C**) ZIKV NS5 levels in the IP samples were quantified and means of protein signals (normalized to IGF2BP2) ± SEM based on three independent experiments are shown. ***: p<0.001 (unpaired t-test).

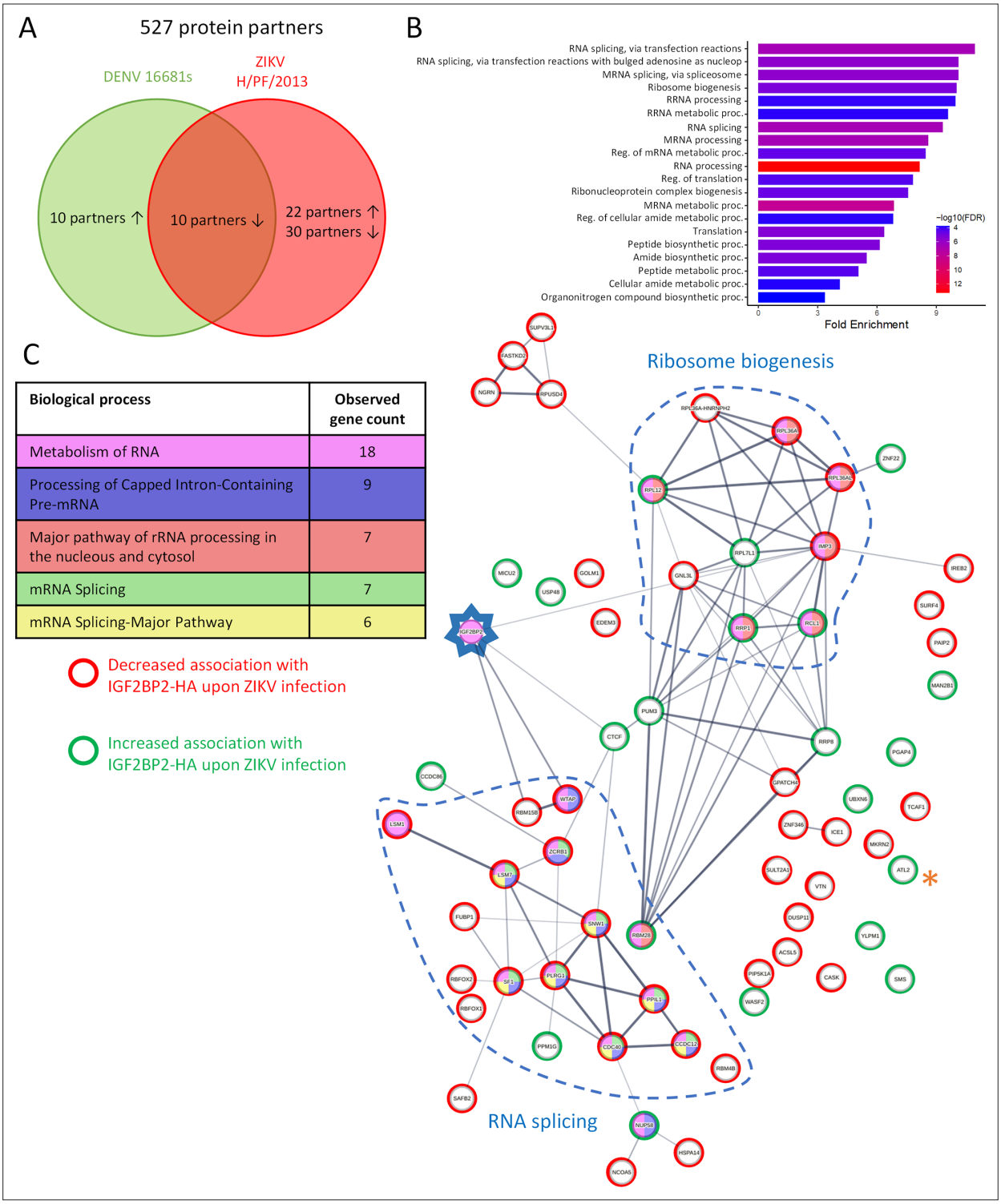

Biological process	Observed gene count
Metabolism of RNA	18
Processing of Capped Intron-Containing Pre-mRNA	9
Major pathway of rRNA processing in the nucleous and cytosol	7
mRNA Splicing	7
mRNA Splicing-Major Pathway	6

Figure 9. Zika virus (ZIKV) infection alters the IGF2BP2 proteo-interactome. Huh7.5 cells expressing IGF2BP2-HA and control cells were infected with ZIKV H/PF/2013, dengue virus serotype 2 (DENV2) 16681s, or left uninfected. Two days later, cell extracts were prepared and subjected to anti-HA immunoprecipitations. Resulting complexes were analyzed by quantitative mass spectrometry. (**A**) Venn diagram depicting the overlap between IGF2BP2 partners modulated by ZIKV and/or DENV infections. (**B**) Gene ontology (GO) biological process analyses of the IGF2BP2 interactions which were impacted upon ZIKV infection. (**C**) Interaction tree of the 62 IGF2BP2 interactions modulated by ZIKV infection (generated with STRING online resource). The red and green circles identify the partners of the STRING network whose association with IGF2BP2 is decreased and increased during infection, respectively. The biological process analysis generated by STRING is also shown.

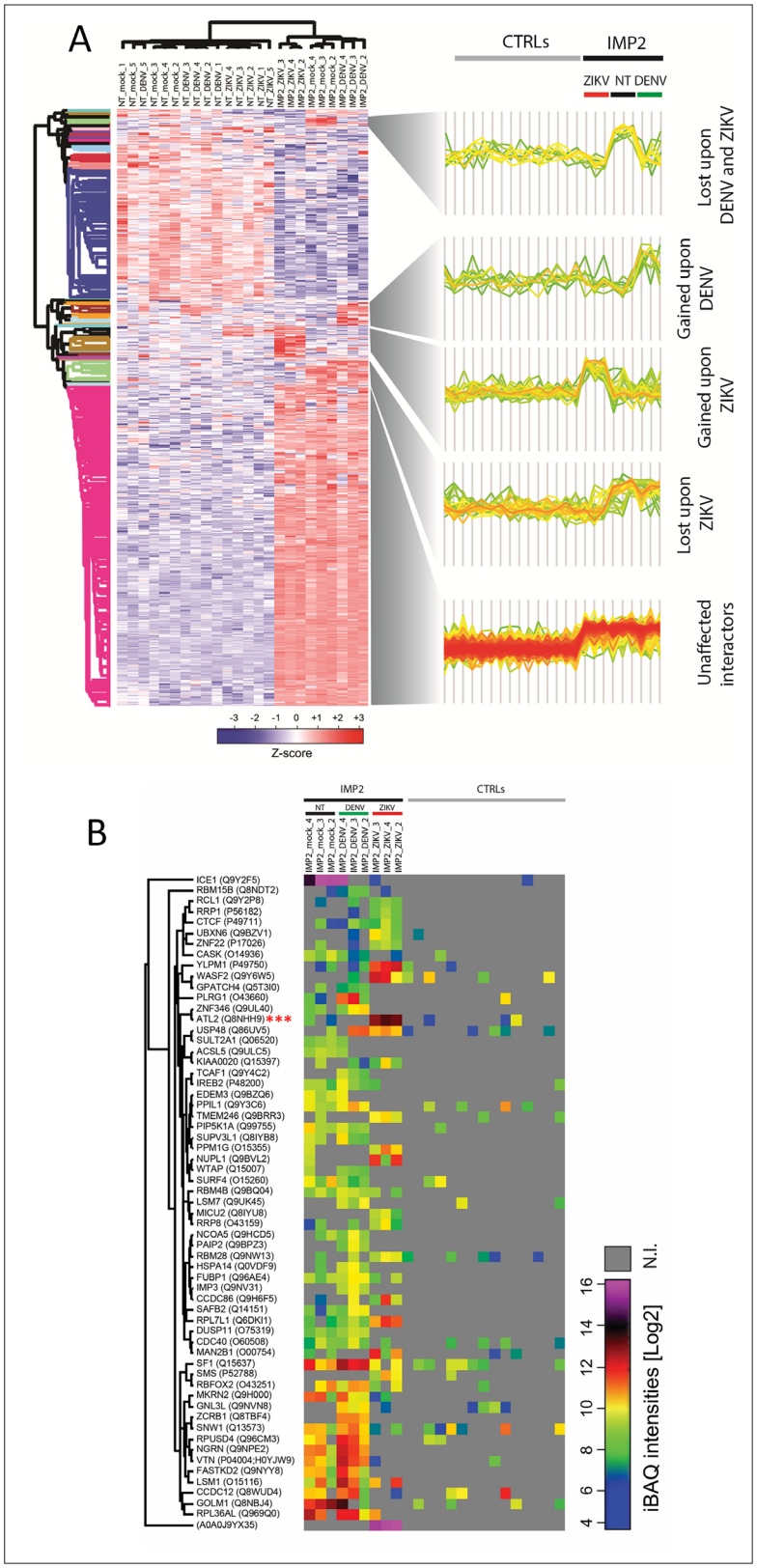

Figure 9—figure supplement 1. Orthoflavivirus infection modulates the interactome of IGF2BP2. (**A**) Heatmap of z-scored protein intensities of all significantly regulated interacting proteins (ANOVA, false discovery rate [FDR] < 0.05) across stimuli (mock, dengue virus [DENV]-infected, Zika virus [ZIKV]-infected) and baits (nontarget [NT], IGFBP2). (**B**) Intensity-based absolute quantification (iBAQs) of protein abundance of differential interacting proteins of IGF2BP2 upon DENV or ZIKV infection (N.I.=not identified).

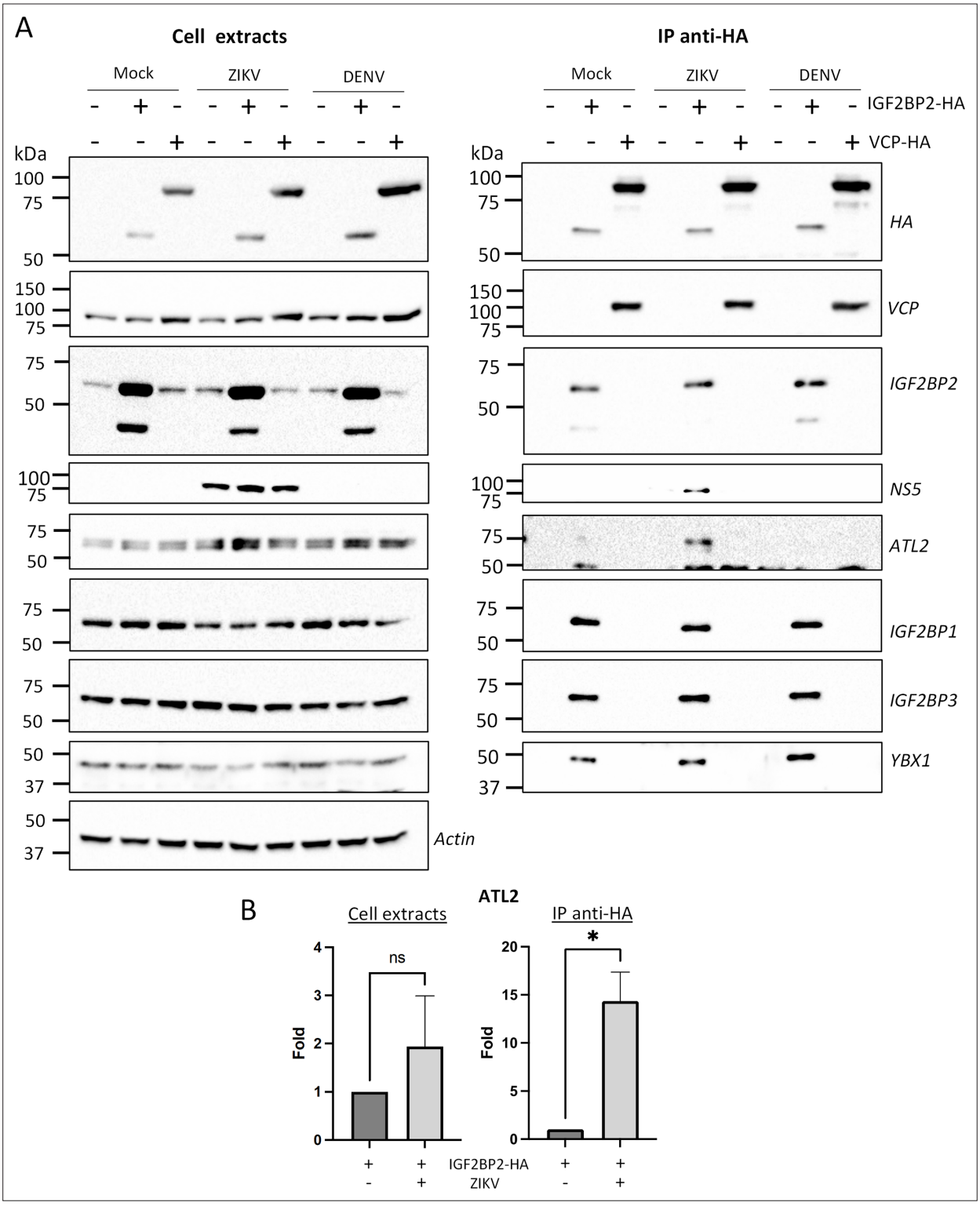

Figure 9—figure supplement 2. Zika virus (ZIKV) infection enhances the interaction between IGF2BP2 and ATL2. (**A**) Huh7.5 cells expressing IGF2BP2-HA and control cells were infected with ZIKV H/PF/2013 at an MOI of 10 or left uninfected. Two days later, cell extracts were prepared and subjected to anti-HA immunoprecipitations. The resulting complexes were analyzed by western blotting for their abundance in the indicated proteins. (**B**) ATL2 levels were quantified and means of protein signals (normalized to actin [extracts] and IGF2BP2 [IP]) ± SEM are shown. *: p<0.05; ns: not significant (unpaired t-test).

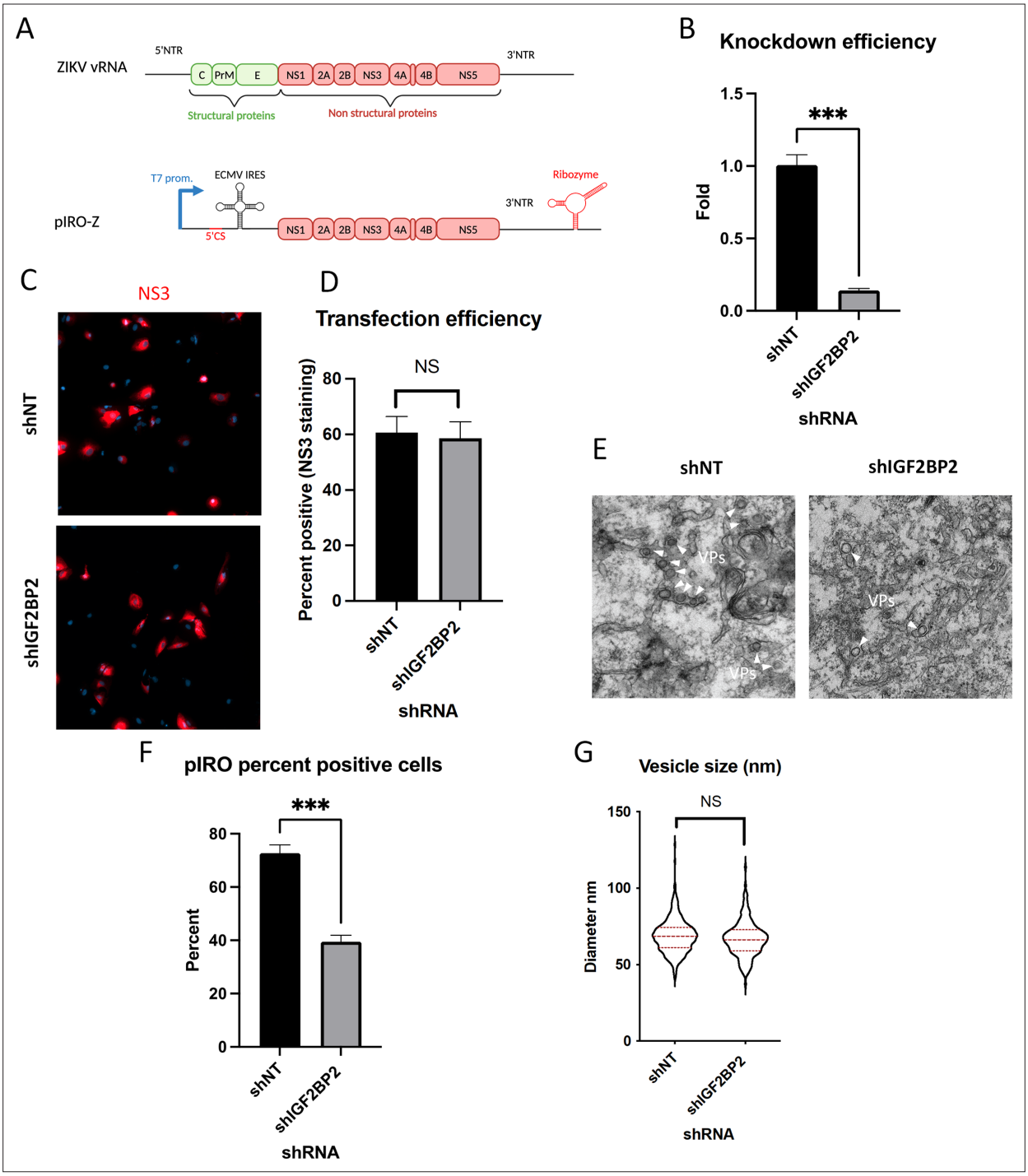

Figure 10. IGF2BP2 regulates the biogenesis of Zika virus (ZIKV) replication organelles. (**A**) Schematic representation of the pIRO system. Upon transfection in cells expressing the T7 RNA polymerase, this plasmid allows the cytoplasmic transcription of NS1-NS5 polyprotein under the control of T7 promoter, in a ZIKV replication-independent manner. NS1-5 polyprotein synthesis is under the control of ECMV IRES. The presence of both ZIKV 3′ NTR and 5′ cyclization sequence (5′ CS) is required for efficient vesicle packet (VP) induction. Finally, the activity of HDV ribozyme ensures that the 3′ terminus of the RNA is similar to that of viral RNA (vRNA) genome. Huh7-Lunet-T7 were transduced with short-hairpin RNA (shRNA)-expressing lentiviruses at an MOI of 5–10. Two days later, transduced cells were transfected with pIRO-Z plasmid. Sixteen hours later, cells were analyzed for (**B**) IGF2BP2 mRNA levels by RT-qPCR to measure knockdown efficiency, (**C–D**) transfection efficiency by confocal imaging of NS3-labeled cells, and (**E**) for VP content by transmission electron microscopy. Electron micrographs were used to measure (**F**) the percentage of cells with VPs and (**G**) the diameter of VPs in each condition. ***: p<0.001; NS: not significant (unpaired t-test).

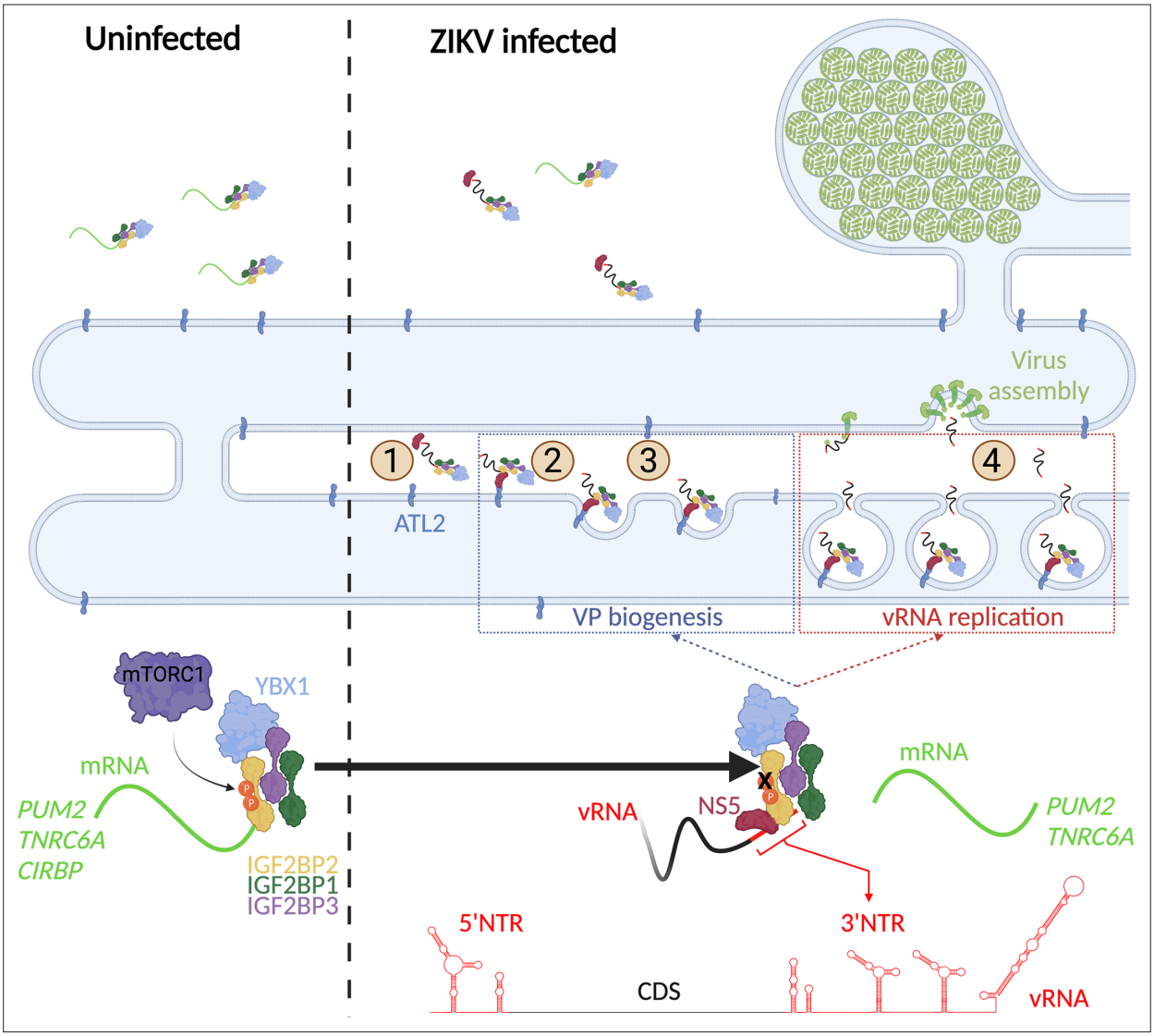

Figure 11. A model for IGF2BP2 involvement in Zika virus (ZIKV) life cycle. Step 1: After NS protein synthesis early after virus entry, IGF2BP2 associates with NS5 and vRNA, thus excluding *PUM2* and *TNRC6A* mRNA from the ribonucleprotein (RNP). Step 2: The infection-induced association between IGF2BP2 RNP and ATL2 allows the targeting of vRNA/NS5 to the endoplasmic reticulum (ER). Step 3: Viral factors and ATL2 induce the bending of the ER membrane and the formation of vesicle packets (VPs) allowing highly processive vRNA synthesis. Step 4: IGF2BP2 might be involved in the packaging of vRNA into assembling viruses by targeting the genome to the VP pore. The recruitment of IGF2BP2 to the replication compartment might be dependent on its mTOR complex 1 (mTORC1)-dependent phosphorylation status.